

## A New Thermodynamic Approach for Protein Partitioning in Reverse Micellar Solution

S. Osfouri<sup>a,\*</sup>, T. Tayebi<sup>a</sup> and R. Azin<sup>b</sup>

<sup>a</sup>Department of Chemical Engineering, Faculty of Petroleum, Gas, and Petrochemical Engineering, Persian Gulf University, Bushehr, Iran

<sup>b</sup>Department of Petroleum Engineering, Faculty of Petroleum, Gas, and Petrochemical Engineering,  
Persian Gulf University, Bushehr, Iran

(Received 27 July 2017, Accepted 4 October 2017)

Reverse micellar systems are nano-fluids with unique properties that make them attractive in high selectivity separation processes, especially for biological compounds. Understanding the phase behavior and thermodynamic properties of these nano-systems is the first step in process design. Separation of components by these nano-systems is performed upon contact of aqueous and reverse micellar phases. Due to the complexities of the molecular interactions of components, phase behavior studies of these solutions are different from regular liquid-liquid systems, and few thermodynamic models have been developed to describe distribution of extract between phases. In this study, a thermodynamic model with  $\phi$ - $\phi$  approach and use of equations of states is developed for the first time to describe the protein phase equilibria in reverse micellar systems. The developed model assumes that some reverse micelles act as active surfaces which can adsorb protein molecules. In addition, the non-ideal behavior of micellar solution was modeled by three equation of states, *i.e.* van der Waals, Peng-Robinson, and Soave-Redlich-Kwong. Results showed that Soave-Redlich-Kwong equation of state shows the best match with experimental data of bovine serum albumin extraction from aqueous solution using reverse micellar solution of cetyltrimethylammonium bromide, a cationic surfactant. In addition, results indicate that the proposed thermodynamic model can describe the changes in electrostatic forces and increase in active surfaces on equilibrium protein extraction. Moreover, the standard deviation shows an excellent match between experimental data and model predictions.

**Keywords:** Thermodynamic model, Reverse micelle, EOS, Extraction, Protein

### INTRODUCTION

Reverse micelles are nano-systems formed by dissolving certain amounts of surfactants in organic solvents [1]. Viscosity of micellar solutions are in the range of organic solvent viscosity and these solutions are thermodynamically stable [2,3]. Although the bulk of micellar solutions are hydrophobic, the aqueous core in the center of such nano-systems make them suitable sites for nano-scale dissolution of hydrophilic materials. This unique property has led to extensive use of reverse micellar systems in special separation processes with high purity and selectivity [4-9].

In addition, the hydrophilic medium is known as "*nano-scale reactor*" for aqueous chemical reactions [10]. One of the key factors in determining the size of reverse micelles is water to surfactant molar ratio,  $w_o$ . Previous studies have focused on producing nano-particles with controlled size in the aqueous core by controlling  $w_o$  [11-14], which has wide application in drug delivery [15,16], industrial catalysts [17-20] and enhanced oil recovery [21,22]. Diverse applications and high value of products have led more attention towards upscaling the processes from bench scale to industrial. The difference between chemical potential of a component in two phases provides the driving force for mass transfer from aqueous phase to the core of reverse micelles [23,24]. The electrostatic forces in these systems are one of the main

\*Corresponding author. E-mail: [osfour@pgu.ac.ir](mailto:osfour@pgu.ac.ir)

mechanisms for mass transfer between phases [25]. Proper understanding the phase behavior of these nano-systems is essential for the process design. Thermodynamic models that describe the phase equilibrium in reverse micellar nano-systems provide the backbone of process development and scale up for downstream processes.

So far, three categories of thermodynamic models have been proposed in this area [26]. The first category is based on Gibbs free energy minimization of equilibrium extraction from aqueous phase to reverse micellar phase. In 1988, Bratko *et al.* modeled the protein extraction from aqueous phase using core-shell model [27]. Bruno *et al.* extended their model by including the interaction between internal charged surface of reverse micelles and host molecule [28]. The second category, also known as “mass action” models, considers a pseudo equilibrium reaction that forms protein-reverse micelle complex. Woll and Hatton proposed the first mass action model in 1989 by correlating forward distribution coefficient with pH of aqueous phase and surfactant concentration [29]. In 2004, Haghtalab and Osfouri developed the previous mass action model by including ionic strength of aqueous phase [30]. Other models of this category are proposed by assuming equality of equilibrium concentration in two phases [31] or application of Pitzer model to account for non-ideal behavior of extract in reverse micellar phase [32]. The third category of models involves simulation of molecular extraction in reverse micellar solutions using adsorption phenomenon. Brandani *et al.* applied this concept to model the protein extraction from aqueous phase using Langmuir adsorption isotherm [33]. In this category, the vacancy solution theory has successfully modeled the non-ideal behavior of reverse micellar solution and extraction process modeling [26].

Contrary to classic liquid-liquid systems, few thermodynamic models are available to describe phase equilibria of reverse micellar systems. Complexity of phase equilibria in nano-fluid reverse micellar systems is attributed to unknown interactions between components in these systems. In this work, a  $\phi$ - $\phi$  approach is developed for the first time to study the non-ideal behavior of extract in reverse micellar solutions using equations of state (EOS). The van der Waals (vdW) [34], Peng-Robinson (PR) [35] and Soave-Redlich-Kwong (SRK) [36] EOSs are used to

model protein distribution of Bovine Serum Albumin (BSA) between aqueous and reverse micellar systems. Moreover, effects of changes in pH and surfactant concentration are studied.

## THERMODYNAMIC MODELING

Based on vacancy solution theory, we assume that the active surface of reverse micelle,  $A$ , acts as a void space and can adsorb protein from aqueous phase. This imaginary void space does not react with adsorbent molecule and is chemically inert. The fraction of covered area,  $\theta_p$ , by adsorbed component,  $n_p$ , in reverse micellar phase,  $rm$ , is calculated as:

$$\theta_p = \left[ \frac{n_p^{(rm)}}{n_p^{(rm)_{max}}} \right] \quad (1)$$

The superscript *max* denotes the maximum moles of adsorbed proteins on the active surface of reverse micelles. The chemical potential of protein in aqueous (*aq*) and reverse micellar (*rm*) phases will be equal at equilibrium conditions:

$$\mu_p^{(rm)} = \mu_p^{(aq)} \quad (2)$$

The non-ideality of equilibrium phases may be written for each component as Eq. (3) [37]:

$$A\pi\theta_p\hat{\phi}_p^{(rm)} = k_{ap}RT\hat{f}_p^{(aq)} \quad (3)$$

where  $\pi$  and  $k_{ap}$  are spreading pressure and protein adsorption isotherm constant, respectively. Besides, the fugacity of protein in aqueous phase,  $\hat{f}_p^{(aq)}$ , is related to the system pressure,  $P$ , protein fugacity coefficient,  $\hat{\phi}_p^{(aq)}$ , and equilibrium composition of adsorbed component in aqueous phase,  $X_p^{(aq)}$ :

$$\hat{f}_p^{(aq)} = X_p^{(aq)}\hat{\phi}_p^{(aq)}P \quad (4)$$

At low protein concentrations, the fugacity coefficient of protein in aqueous phase is assumed unit. Therefore, combining Eqs. (3) and (4) gives the equilibrium

composition of protein in aqueous phase:

$$X_p^{(aq)} = \left( \frac{A\pi}{k_{ap} RTP} \right) \cdot \theta_p^{(rm)} \cdot \widehat{\varphi}_p^{(rm)} \quad (5)$$

Fugacity coefficient of protein in reverse micellar solution is calculated from cubic equations of state. Based on Zhou *et al.* [37], the generic form of EOS for adsorption on active surfaces is written as:

$$\left[ A\pi + \frac{\alpha \cdot (n_p^{(rm)\max})^2}{1 + U\beta n_p^{(rm)\max} + W(\beta n_p^{(rm)\max})^2} \right] \left[ 1 - (\beta n_p^{(rm)\max})^m \right] = n_p^{(rm)\max} RT \quad (6)$$

where  $\alpha$ ,  $\beta$  are EOS parameters and are calculated by using mixing rules:

$$\alpha = \sum_i \sum_j \theta_i \theta_j \alpha_{ij} \quad (7)$$

$$\beta = \sum_i \sum_j \theta_i \theta_j \beta_{ij} \quad (8)$$

where  $\alpha_{ij}$ ,  $\beta_{ij}$  are binary interaction parameters and are calculated from adjustable binary interaction parameters of pure components,  $\alpha_{ii}$ ,  $\alpha_{jj}$ ,  $\beta_{ii}$  and  $\beta_{jj}$ :

$$\alpha_{ij} = \frac{1}{2(\alpha_{ii} + \alpha_{jj})(1 - k_{ij})} \quad (9)$$

$$\beta_{ij} = (\beta_{ii} \beta_{jj})^{0.5} (1 + c_{ij}) \quad (10)$$

The adjustable parameters  $k_{ij}$  and  $c_{ij}$  are generally taken as zero [38]. This situation is termed the "predictive mode", thus:

$$\alpha_{ij} = \alpha_{ji} \quad (11)$$

$$\beta_{ij} = \beta_{ji} \quad (12)$$

Equation (6) is a general EOS form from which well known vdW, PR, and SRK EOSs may be derived. Table 1 summarizes  $m$ ,  $U$  and  $W$  respective to each EOS. Moreover,

other forms of EOSs, such as Eyring and ZGR EOSs, can be obtained by setting constant "m" in Eq. (6) to 1/2 and 1/3, respectively, while  $U$  and  $W$  are equal to zero [37]. The applications of five special forms of two-dimensional EOS were evaluated for several gas adsorption systems. The results showed that the two-dimensional EOS models can be used to fit pure adsorption isotherms more accurately than the Langmuir model, and were applicable to predict gas mixture adsorption, using mixing rules. Besides, all forms of the two-dimensional EOS were capable to represent azeotropic behavior and predictive results for binary mixtures based on pure component data.

Fugacity coefficient of protein in reverse micellar solution can be calculated from Eqs. (13) and using EOS:

$$\ln \widehat{\varphi}_p^{(rm)} = \frac{2 \sum_j \beta_{pj} n_p^{(rm)} - \beta n_p^{(rm)\max}}{1 - \beta n_p^{(rm)\max}} - \frac{1}{m} \ln(1 - \beta n_p^{(rm)\max}) - \ln Z_m + T_1 + T_2 \quad (13)$$

$T_1$  and  $T_2$  are defined by Eqs. (14) and (15):

$$T_1 = - \frac{2\alpha \sum_j \beta_{pj} n_j^{(rm)} - \alpha \beta n_p^{(rm)\max}}{RT\beta [1 + U\beta n_p^{(rm)\max} + W(\beta n_p^{(rm)\max})^2]} \quad (14)$$

(15)

$Z_m$  is compressibility factor which can be calculated from Eq. (16):

$$Z_m = \frac{A\pi}{RTn_p^{(rm)\max}} \quad (16)$$

Combining Eqs. (16), (5), and using the definition of  $\theta_p$ , Eq. (17) is obtained:

$$X_p^{(aq)} = Z_m \left( \frac{n_p^{(rm)}}{k_{ap} \cdot P} \right) \widehat{\varphi}_p^{(rm)} \quad (17)$$

Generally, distribution coefficient,  $K$ , defined as the ratio of protein concentrations in reverse micellar solution  $[P]^{(rm)}$

**Table 1.** Numerical Values of Different EOS Parameters

Equation of State	m	U	W
vdW	1	0	0
PR	1	2	-1
SRK	1	1	0

**Table 2.** Comparison of Global Optimization Results with VST Model

Model	VST [1]	vdW EOS	PR EOS	SRK EOS
$\sigma$	0.134	0.129	0.127	0.122
AAD (%)	10.56	10.66	8.35	7.85

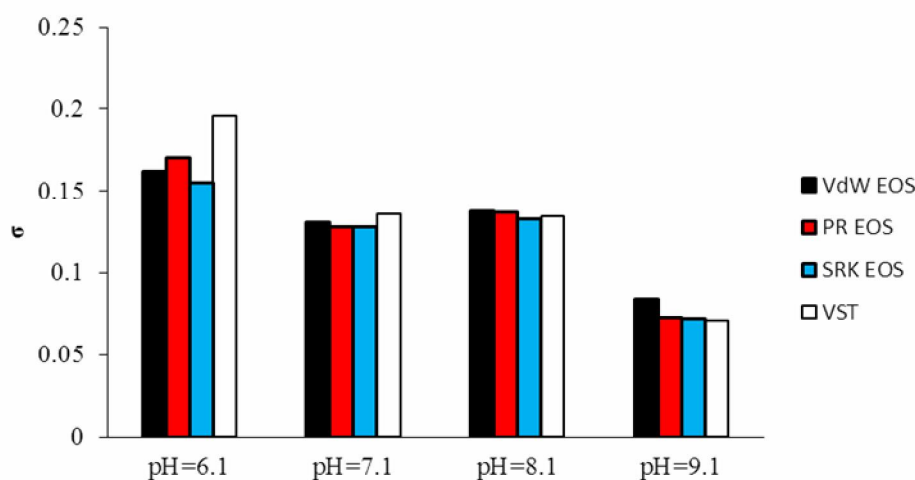


**Fig. 1.** Standard deviation comparison of different EOSs and VST model at four aqueous pH levels.

and aqueous phase  $[P]^{(aq)}$ , is used to evaluate extraction efficiency:

$$K = \frac{[P]^{(rm)}}{[P]^{(aq)}} = \frac{n_p^{(rm)}}{n_p^{(aq)}} \times \frac{V^{(aq)}}{V^{(rm)}} \quad (18)$$

where  $V_{(aq)}/V_{(rm)}$  is volumetric ratio of aqueous phase to reverse micellar phase. In addition, the protein mole fraction

in aqueous phase is related to protein concentration (mM) in this phase,  $[P]^{(aq)}$ , based on the mass balance equation:

$$X_p^{(aq)} = \frac{n_p^{(aq)}}{n_p^{(aq)} + n_w^{(aq)}} = \frac{[P]^{(aq)}}{[P]^{(aq)} + 55555.5} \quad (19)$$

where  $n_w^{(aq)}$  is the total moles of solvent in aqueous phase.

Equation (17) accompanied with Eqs. (18) and (19) can be used with any EOS to determine respective terms of fugacity coefficient and compressibility factor and perform phase equilibrium calculations. The proposed thermodynamic model contains adjustable parameters as binary interaction parameters, coefficient of adsorption isotherm, and maximum moles of protein on the surface of reverse micelles. The global standard deviation of predictions, defined by Eq. (20), was used as the objective function to obtain the optimized adjustable parameters for each EOS:

$$\sigma = \left( \frac{\sum_i^N \left( \frac{K_i^{\text{exp}} - K_i^{\text{cal}}}{K_i^{\text{exp}}} \right)^2}{N} \right)^{0.5} \quad (20)$$

where  $N$  is all experimental data including all protein partition coefficients at two surfactant concentration levels and four aqueous pH levels.

## RESULTS AND DISCUSSION

The capability of the model was examined using experimental data of BSA ( $M_w = 67000$  Da,  $pI = 4.7$ ) partitioning between aqueous phase and reverse micellar phase [26]. The reverse micellar phase is composed of isooctane-1-hexanol (4/1 volumetric ratio) and cationic cetyltrimethylammonium bromide (CTAB) surfactant. As the surface of reverse micelle is composed of cationic surfactant, the maximum mole of protein is a function of surfactant concentration and pH of aqueous phase. Thus, the effects of surfactant concentration and pH of aqueous phase on protein partitioning was studied at two levels (20 and 30 mM concentration) and four levels (6.1, 7.1, 8.1 and 9.1), respectively. Besides, KCl with concentration of 0.1 molar was used to fix the ionic strength of protein-containing aqueous phase. Moreover, the volumetric ratio of aqueous phase to reverse micellar phase was fixed at one. Model global optimization was performed using Levenberg-Marquardt [39] algorithm, and results together with absolute average deviation (AAD

$$AAD(\%) = \frac{1}{N} \sum_{i=1}^N \left( \frac{100 \times |K_i^{\text{exp}} - K_i^{\text{cal}}|}{K_i^{\text{exp}}} \right)$$

) are shown in Table 2 for three EOSs. The global optimization applied on all protein partition coefficients at two surfactant concentration levels, and four pH levels for each EOS separately. The calculated results of vacancy solution theory (VST) as a successful model for phase equilibria of protein distribution between reverse micellar and in aqueous phases [26] are also given for comparison. In addition, standard deviation of results for each pH of aqueous solution and two surfactant concentration levels is shown in Fig. 1.

Both VST model and the new model have the same number of adjustable parameters. Results showed that the developed model by SRK has the least standard deviation compared to other EOSs and VST model for all pH ranges. In addition, the results showed that by increasing the non-ideality of solutions, due to increasing pH of aqueous solution from 8.1 to 9.1 and consequently increasing attractions between cationic reverse micelles and negative charged proteins, the VST model and the developed model by SRK are more successful for predictions of protein partition coefficients. Figure 2 shows variations in BSA distribution coefficient with respect to equilibrium protein concentration in aqueous phase at four pH levels of aqueous phase. The solid line represents the calculated results by model based on SRK EOS. By increasing pH of aqueous phase and deviation from protein pI, accumulation of negative charges increases on protein surface. This increases the electrostatic forces between protein and active surfaces of cationic reverse micellar solution, which results in the increase in protein distribution coefficient. As shown in Fig. 2, the developed thermodynamic model can predict effect of surfactant concentration for both levels. Table 3 gives maximum absorbable moles of protein on the active surfaces of reverse micellar solutions. The main driving force for protein transfer from aqueous phase to reverse micellar solution is electrostatic interactions; therefore, it is expected that by increasing pH of aqueous phase, while keeping the surfactant concentration, the number of protein-adsorbing active sites increases, as can be seen in Table 3. In addition, at fixed electrostatic forces and by increasing the number of reverse micelles that results from increase in surfactant concentration, the adsorption active surface

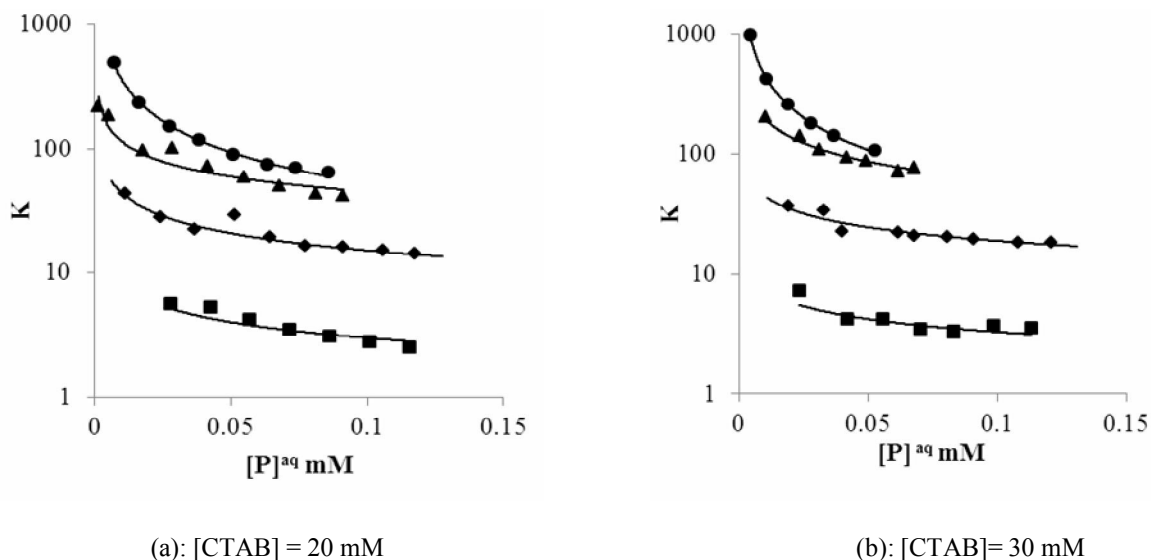


**Fig. 2.** BSA partition coefficient at four pH levels (solid line: Model, Label: Exp. data [1]: ■: pH = 6.1, ◆: pH = 7.1, ▲: pH = 8.1, ●: pH = 9.1) using SRK EOS.

**Table 3.** The Maximum Number of Moles of Protein Adsorbed on the Active Surface of Reverse Micelles at Different Aqueous pH Solutions and Surfactant Concentrations

[CTAB]	pH			
	6.1	7.1	8.1	9.1
20 mM	0.398	3.261	12.140	19.890
30 mM	0.399	3.947	18.200	20.880

increases, resulting in the increase in the maximum extracted moles. This is also shown in Table 3 for two concentration levels. Details of binary interaction parameters are given in the appendix.

## CONCLUSIONS

In this study, a thermodynamic model was developed by combining theory of protein molecule adsorption on hypothetical active surfaces with classic  $\phi$ - $\phi$  approach of EOS to describe the extraction process by the reverse micellar systems. Results showed that the proposed model

can predict the equilibrium behavior of such special liquid-liquid systems. The lower standard deviation of proposed model predictions compared to VST model indicates better agreement between model and experimental data. Sensitivity analysis showed that the SRK EOS is superior over vdW and PR EOSs for predicting the equilibrium conditions in aqueous-reverse micellar phases. The proposed model is flexible upon changes in electrostatic forces caused by increase in pH of aqueous phase and increase in negative charges on protein surfaces. Results showed that the model is applicable for a wide range of pH. Moreover, the proposed model can predict the increase in

distribution coefficient due to increase in the active sites that form at higher surfactant concentrations. In addition, the model matches well with changes in electrostatic forces.

## NOMENCLATURE

A	Surface area per mass of adsorbent, (cm) <sup>2</sup> kg <sup>-1</sup>
c	Parameter in Eq. (10)
$\hat{f}$	Fugacity of component in a mixture, bar cm
K	Partition coefficient
k	Parameter in Eq. (9)
$k_{a_i}$	Slope of isotherm of component <i>i</i>
M	Coefficient of generic equation of state
N	Number of experimental data
N	Number of adsorbed moles per gram of adsorbent, (m mol g <sup>-1</sup> )
P	Pressure (bar)
[P]	Protein concentration (mM)
R	Universal gas constant, bar cm <sup>3</sup> (mol <sup>-1</sup> K <sup>-1</sup> )
T	Temperature (K)
U	Coefficient of generic equation of state
W	Coefficient of generic equation of state
X	Mole fraction of component

### Greek Letter

$\alpha$	EOS model constant, (bar cm <sup>3</sup> g)/mol mmol)
$\beta$	EOS model constant (g mmol <sup>-1</sup> )
$\theta$	Fractional coverage of active surface
$\mu$	Chemical potential (J mol <sup>-1</sup> )
$\pi$	Spreading pressure (bar cm)
$\sigma$	Standard deviation
$\hat{\varphi}$	Fugacity coefficient of component in mixture

### Superscript

<i>aq</i>	Aqueous phase
<i>cal</i>	Calculated
<i>exp</i>	Experimental

<i>max</i>	Maximum
<i>rm</i>	Reverse micellar phase

### Subscript

<i>I</i>	Component
<i>J</i>	Component
<i>P</i>	Protein

## REFERENCES

- [1] Melo, E. P.; Aires-Barros, M. R.; Cabral, J. M. S., Reverse micelles and protein biotechnology. *Biotechnol. Annu. Rev.* **2001**, *7*, 87-129, DOI: 10.1016/S1387-2656(01)07034-X.
- [2] Narang, A. S.; Delmarre, D.; Gao, D., Stable drug encapsulation in micelles and microemulsions. *Int. J. Pharm.* **2007**, *345*, 9-25, DOI: 10.1016/j.ijpharm.2007.08.057.
- [3] Stano, P.; Luisi, P. L., Self-reproduction of micelles, reverse micelles, and vesicles: compartments disclose a general transformation pattern. *Advances in Planar Lipid Bilayers and Liposomes* **2008**, *7*, 221-263, DOI: 10.1016/S1554-4516(08)00009-4.
- [4] Zhang, W.; Liu, X.; Fan, H.; Zhu, D.; Wu, X.; Huang, X.; Tang, J., Separation and purification of alkaloids from *Sophora flavescens* Ait. by focused microwave-assisted aqueous two-phase extraction coupled with reversed micellar extraction. *Ind. Crops Prod.* **2016**, *86*, 231-238, DOI: 10.1016/j.indcrop.2016.03.052.
- [5] Gaikawai, R. P.; Wagh, S. A.; Kulkarni, B. D., Extraction and purification of tannase by reverse micelle system. *Sep. Purif. Technol.* **2012**, *89*, 288-296, DOI: 10.1016/j.seppur.2012.01.043.
- [6] Reddy, T. R.; Meeravali, N. N.; Reddy, A. V. R., Novel reverse mixed micelle mediated transport of platinum and palladium through a bulk liquid membrane from real samples. *Sep. Purif. Technol.* **2013**, *103*, 71-77, DOI: 10.1016/j.seppur.2012.10.025.
- [7] Mandal, S.; De, S., Copper nanoparticles in AOT "revisited"-direct micelles versus reverse micelles. *Mater. Chem. Phys.* **2016**, *183*, 410-421, DOI: 10.1016/j.matchemphys.2016.08.046.
- [8] Krieger, N.; Taipa, M. A.; Aires-Barros, M. R.; Melo, E. H. M.; Lima-Filho, J. L.; Cabral, J. M. S.,

- Purification of penicillium citrinum lipase using AOT reverse micelles. *J. Chem. Technol. Biotechnol.* **1997**, *69*, 77-85, DOI: 10.1002/(SICI)1097-4660(199705)69:1<77::AID-JCTB666>3.0.CO;2-V.
- [9] Storm, S.; Aschenbrenner, D.; Smirnova, I., Reverse micellar extraction of amino acids and complex enzyme mixtures. *Sep. Purif. Technol.* **2014**, *123*, 23-34, DOI: 10.1016/j.seppur.2013.11.035.
- [10] Noh, J.; Yi, M.; Hwang, S.; Im, K. M.; Yu, T.; Kim, J., A facile synthesis of rutile-rich titanium oxide nanoparticles using reverse micelle method and their photocatalytic applications. *J. Ind. Eng. Chem.* **2016**, *33*, 369-373, DOI: 10.1016/j.jiec.2015.10.020.
- [11] Ghiaci, M.; Aghaei, H.; Abbaspur, A., Size-controlled synthesis of ZrO<sub>2</sub>-TiO<sub>2</sub> nanoparticles prepared via reverse micelle method: Investigation of particle size effect on the catalytic performance in vapor phase Beckmann rearrangement. *Mater. Res. Bull.* **2008**, *43*, 1255-1262, DOI: 10.1016/j.materresbull.2007.05.022.
- [12] Osfour, S.; Azin, R.; Pakdaman, E., Dynamics of water state in nanoconfined environment. *J. Taiwan Inst. Chem. Eng.* **2014**, *45*, 828-832, DOI: 10.1016/j.jtice.2013.09.008.
- [13] Yao, L.; Xu, G.; Dou, W.; Bai, Y., The control of size and morphology of nanosized silica in Triton X-100 based reverse micelle. *Colloids Surf., A: Physicochem. Eng. Aspects* **2008**, *316*, 8-14, DOI: 10.1016/j.colsurfa.2007.08.016.
- [14] Perez-Coronado, A. M.; Calvo, L.; Alonso-Morales, A.; Heras, F.; Rodrigues, J. J.; Gilarranz, M. A., Multiple approaches to control and assess the size of Pd nanoparticles synthesized via water-in-oil microemulsion. *Colloids Surf., A: Physicochemical and Engineering Aspects* **2016**, *497*, 28-34, DOI: 10.1016/j.colsurfa.2016.02.012.
- [15] Du, Y. Z.; Wang, L.; Yuan, H.; Hu, F. Q., Linoleic acid-grafted chitosan oligosaccharide micelle for intracellular drug delivery and reverse drug resistance of tumor cells. *Int. J. Biol. Macromol.* **2011**, *48*, 215-222, DOI: 10.1016/j.ijbiomac.2010.11.005.
- [16] Koyamatsu, Y.; Hirano, T.; Kakizawa, Y.; Okano, F.; Takarada, T.; Maeda, M., pH-responsive release of proteins from biocompatible and biodegradable reverse polymer micelles. *J. Controlled Release* **2014**, *173*, 89-95, DOI: 10.1016/j.jconrel.2013.10.035.
- [17] Osakoo, N.; Henkel, R.; Loiha, S.; Roessner, F.; Wittayakun, J., Palladium-promoted cobalt catalysts supported on silica prepared by impregnation and reverse micelle for Fischer-Tropsch synthesis. *Appl. Catal., A: General* **2013**, *464-465*, 269-280, DOI: 10.1016/j.apcata.2013.06.008.
- [18] Cheney, B. A.; Lauterbach, J. A.; Chen, J. G., Reverse micelle synthesis and characterization of supported Pt/Ni bimetallic catalysts on  $\gamma$ -Al<sub>2</sub>O<sub>3</sub>. *Appl. Catal., A: General* **2011**, *394*, 41-47, DOI: 10.1016/j.apcata.2010.12.021.
- [19] Limaye, M. V.; Singh, S. B.; Das, R.; Poddar, P.; Abyaneh, M. K.; Kulkarni, S. K., Magnetic studies of SiO<sub>2</sub> coated CoFe<sub>2</sub>O<sub>4</sub> nanoparticles. *J. Magn. Magn. Mater.* **2017**, *441*, 683-690, DOI: 10.1016/j.jmmm.2017.06.061.
- [20] Noh, J.; Yi, M.; Hwang, S.; Im, K. M.; Yu, T.; Kim, J., A facile synthesis of rutile-rich titanium oxide nanoparticles using reverse micelle method and their photocatalytic applications. *J. Ind. Eng. Chem.* **2016**, *33*, 369-373, DOI: 10.1016/j.jiec.2015.10.020.
- [21] Wu, Y.; Chen, W.; Dai, C.; Huang, Y.; Li, H.; Zhao, M.; He, L.; Jiao, B., Reducing surfactant adsorption on rock by silica nanoparticles for enhanced oil recovery. *J. Pet. Sci. Eng.* **2017**, *153*, 283-287, DOI: 10.1016/j.petrol.2017.04.015.
- [22] Mohammed, M.; Badadagli, T., Wettability alteration: A comprehensive review of materials/methods and testing the selected ones on heavy-oil containing oil-wet systems. *Adv. Colloid Interface Sci.* **2015**, *220*, 54-77, DOI: 10.1016/j.cis.2015.02.006.
- [23] Leodidis, E. B.; Hatton, T. A., Amino acid in AOT reversed micelles. 1. Determination of interfacial partition coefficients using the phase-transfer method. *J. Phys. Chem.* **1990**, *94*, 6400-6411, DOI: 10.1021/j100379a046.
- [24] Hurter, P. N.; Scheutjens, J. M. H. M.; Hatton, T. A., Molecular modeling of micelle formation and solubilization in block copolymer micelles. 2. Lattice theory for monomers with internal degree of freedom. *Macromolecules* **1993**, *26*, 5030-5040, DOI: 10.1021/ma00071a008.
- [25] Krei, G. A.; Hustedt, H., Extraction of enzymes by

- reverse micelles. *Chem. Eng. Sci.* **1992**, *47*, 99-111, DOI: 10.1016/0009-2509(92)80204-P.
- [26] Haghtalab, A.; Osfouri, S., Vacancy solution theory for Partitioning of protein in reverse-micellar systems. *Sep. Sci Technol.* **2003**, *38*, 553-569, DOI: 10.1081/SS-120016651.
- [27] Bratko, D.; Luzar, A.; Chen, S. H., Electrostatic model for protein/reverse micelle complexation. *J. Chem. Phys.* **1988**, *89*, 545-550, DOI: 10.1063/1.455443.
- [28] Bruno, P.; Caselli, M.; Luisi, P. L.; Maestro, M.; Traini, A., A simplified thermodynamic model for protein uptake by reverse micelles: Theoretical and experimental results. *J. Phys. Chem.* **1990**, *94*, 5908-5917, DOI: 10.1021/j100378a056.
- [29] Woll, J. M.; Hatton, T. A., A simple phenomenological thermodynamic model for protein partitioning in reverse micellar systems. *Bioprocess Eng.* **1989**, *4*, 193-199, DOI: 10.1007/BF00369172.
- [30] Haghtalab, A.; Osfouri, S., A simple complexation model and the experimental data for protein extraction using reverse micellar systems. *Iranian J. Biotechnol.* **2004**, *2*, 106-112.
- [31] Rabie, H. R.; Vera, J. H., A simple model for reverse micellar extraction of proteins. *Sep. Sci. Technol.* **1998**, *33*, 1181-1193, DOI: 10.1080/01496399808545248.
- [32] Ashrafizadeh, S. N.; Khoshkbarchi, M. K., Modeling and experimental data for the reverse micellar extraction of proteins using a new surfactant. *Sep. Sci. Technol.* **1998**, *33*, 2579-2592, DOI: 10.1080/01496399808545320.
- [33] Brandani, S.; Brandani, V.; Giacomo, G. D., A thermodynamic model for protein partitioning in reverse micellar systems. *Chem. Eng. Sci.* **1994**, *49*, 3681-3686, DOI: 10.1016/0009-2509(94)00182-0.
- [34] van der Waals, J. D., On the continuity of the liquid and gaseous state. PhD dissertation, Sigthoff U. Leiden, 1873.
- [35] Peng, D. Y.; Robinson, D. B., A new two-constant equation of state. *Ind. Eng. Chem. Fund.* **1976**, *15*, 59-64, DOI: 10.1021/i160057a011.
- [36] Soave, G., Equilibrium constants from a modified Redlich-Kwong equation of state. *Chem. Eng. Sci.* **1972**, *27*, 1197-1340, DOI: 10.1016/0009-2509(72)80096-4.
- [37] Zhou, C.; Hall, F.; Gasem, K. A. M.; Robinson Jr, R. L., Predicting gas adsorption using two-dimensional equation of state. *Ind. Eng. Chem. Res.* **1994**, *33*, 1280-1289, DOI: 10.1021/ie00029a026.
- [38] Gao, G.; Daridon, J. L.; Saint-Guirons, H.; Xans, P., A simple correlation to evaluate binary interaction parameters of the Peng-Robinson equation of state: binary light hydrocarbon systems. *Fluid Phase Equilib.* **1992**, *74*, 85-93, DOI: 10.1016/0378-3812(92)85054-C.
- [39] Chandler, J. P., MARQ 2.3, A. N. S. I. Standard Fortran 1985, Oklahoma State University: Stillwater Oklahoma.